CHAPTER 184

BEM-FEM COMBINED ANALYSIS OF NONLINEAR INTERACTION BETWEEN WAVE AND SUBMERGED BREAKWATER

N.Mizutani[1] , W.G. McDougal[2], A.M. Mostafa[3]

ABSTRACT:

A combined BEM-FEM model has been developed to study the nonlinear dynamic interaction between a submerged breakwater and waves. The resistance coefficients in the equations of motion inside the porous media have been experimentally determined based on measured values of the wave forces on spherical armor units in a submerged breakwater. Comparisons of the numerical model results with the experimental measurements indicate that this modification has improved the model accuracy in simulating the wave deformation and the energy dissipation due to a submerged breakwater. Results also show that the model gives good estimates for the wave kinematics inside and around the breakwater which are necessary to compute the stable armor stone weight.

INTRODUCTION:

Submerged breakwaters have several advantages over the conventional surface piercing structures including aesthetics, less impact on the near shore water quality and ability to trigger early wave breaking. Their use is also recommended on recreational beaches to ensure safe conditions. They are usually constructed from rubble and may be protected by an armor layer of large stones or concrete blocks.

Earlier researchers focused on wave deformation and energy dissipation due to submerged breakwaters, but less interest was given to their internal properties and shape. Driscoll et al. (1992) studied the harmonic generation and transmission past

[1] Assoc. Prof., D.Eng., Dept. of Civil Eng., Nagoya University, Nagoya 464-01, Japan
[2] Prof., Dept. of Civil Eng., Oregon State Univ., Corvallis, OR 97331, USA
[3] Graduate student, M.Eng., Dept. of Civil Eng., Nagoya University, Nagoya 464-01, Japan

a submerged impermeable rectangular obstacle. They conducted laboratory experiments and compared the results with a linear scattering model and a fully nonlinear model. Cruz et al (1992) derived a set of nonlinear vertically integrated equations similar to that of Boussinesq to estimate the wave transformations past a submerged permeable breakwater. They found that their equations work well in the region of cnoidal waves, but the transmitted and the broken wave characteristics could not be well predicted. Gu and Wang (1992) linearized the porous flow equations inside the submerged breakwater using the equivalent energy principle and developed a model based on the Boundary Equation Method (BEM). They found that maximum wave energy dissipation can be achieved at practical permeability levels.

Based on modified Navier-Stokes equations, McCorquodale and Hannoura (1978) developed the flow equations inside the porous media and applied them to the case of rubble mound breakwaters. A mixed numerical model was also developed to simulate the wave motion inside rubble mound breakwaters and, hence, check the stability of the seaward slope (Hannoura and McCorquodale, 1985). Ohyama and Nadaoka (1991) developed an idealized numerical wave tank consisting of sponge layer(s) and the non-reflective wave source developed by Brorsen and Larsen (1987). They used the BEM and proved that their proposed wave tank is applicable for use with irregular and nonlinear wave fields.

Sakakiyama et al. (1991) developed a porous body model analysis of nonlinear wave transformations to study the velocity, pressure fields and free surface displacement in and near rubble mound and composite breakwaters. They considered the flow to be rotational inside and outside the porous media, but their numerical model required a very long CPU run-time. Moreover, in a comparison between permeable and impermeable submerged breakwaters, it has been found that the wave reduction is slightly affected by the porosity of the breakwater (Sakakiyama, 1992).

For wide crown submerged breakwaters, the flow velocities and the wave field behind the breakwater are small and assuming irrotationality of the flow in the wave field may be reasonable. This will reduce the computation time and cost. Therefore, a hybrid-type numerical model has been developed and used to simulate the non-linear dynamic interaction between waves and rectangular permeable submerged breakwater considering irrotational flow in the wave field, but rotational flow inside the porous media (Mizutani et al., 1995).

This study has been conducted to develop an accurate numerical model for the simulation of the nonlinear dynamic interaction between waves and submerged breakwater with irregular cross section. An idealized wave tank, similar to that of Ohyama and Nadaoka (1991), has been used to simulate the nonlinear wave field. Modified Navier-Stokes equations have been employed to simulate the flow inside the porous media (McCorquodale and Hannoura, 1978). The Boundary Element Method (BEM) has been used to develop a numerical model for the wave field.

The Finite Element Method (FEM), based on the weighted residual technique, has been used to solve the flow problem inside the submerged breakwater. The link between the two models has been maintained through boundary conditions on the interface between the wave and porous media fields. The BEM-FEM model computes the wave deformations and the flow inside the submerged breakwater simultaneously at each time step in a time marching scheme.

The resistance coefficients in Navier-Stokes equations have been modified through comparison with a Morison type equation for evaluating the wave forces on a spherical armor unit. The measured values of the wave forces and velocities in the experiments (Mizutani et al., 1994) have been used to estimated the drag and inertia coefficients.

GOVERNING EQUATIONS AND MODEL DEVELOPMENT

Wave Field
The flow in the wave field has been assumed to be irrotational and the water is considered inviscid and incompressible. The idealised wave tank used in this study is shown in Fig.1 and it is governed by the following Poisson equation (Brorsen and Larsen, 1987).

$$\frac{\partial^2 \phi}{\partial X^2} + \frac{\partial^2 \phi}{\partial Z^2} = q^* \tag{1}$$

$$q^* = U^*(Z, t)\delta(X - X_s) \tag{2}$$

where ϕ is the velocity potential; X and Z are the horizontal and vertical coordinates, respectively; q^* corresponds to the flux density at the wave-making source and is zero elsewhere; U^* is the flux density at the wave-making source; δ is Dirac's delta function and X_s is the X-position of the wave-making source. Eq.1 is subjected to the following boundary conditions (see Fig.1):
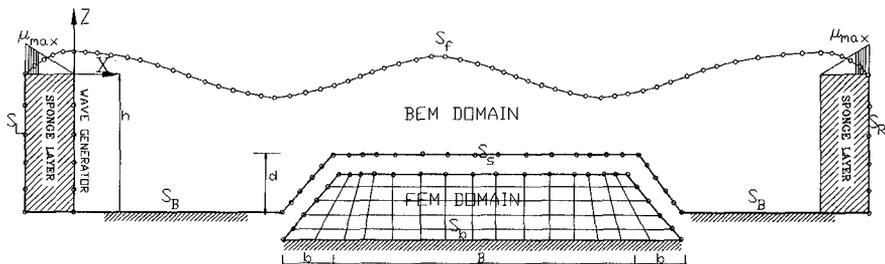

Fig.1 Wave tank for wave-submerged breakwater dynamic interaction

$$\frac{\partial \phi}{\partial n} = n_z \frac{\partial \eta}{\partial t} \qquad \text{(on } S_f) \quad (3)$$

$$\frac{\partial \phi}{\partial n} = 0 \qquad \text{(on } S_B) \quad (4)$$

$$\frac{\partial \phi}{\partial n} = V_n \qquad \text{(on } S_s) \quad (5)$$

$$\frac{\partial \phi}{\partial t} + \frac{1}{2}(\nabla \phi)^2 + g\eta + \mu\phi - \int_{X_1}^{X} \frac{\partial \mu}{\partial X}\phi dX = 0 \qquad \text{(on } S_f) \quad (6)$$

$$\frac{\partial \phi}{\partial X} = \frac{1}{\sqrt{gh}}(\frac{\partial \phi}{\partial t} + \mu\phi + \int_{X_2}^{X_1} \frac{\partial \mu}{\partial X}\phi dX) \qquad \text{(on } S_L) \quad (7)$$

$$\frac{\partial \phi}{\partial X} = -\frac{1}{\sqrt{gh}}(\frac{\partial \phi}{\partial t} + \mu\phi - \int_{X_3}^{X_4} \frac{\partial \mu}{\partial X}\phi dX) \qquad \text{(on } S_R) \quad (8)$$

$$\mu_{max} = (0.25 \sim 0.50)\sqrt{\frac{g}{h}} \qquad (9)$$

where n_z is the directional cosine of the normal outward from the boundary with the Z axis; t is time; V_n/m is the porewater velocity normal to the boundary; m is the porosity; h is the water depth; and η is the water surface elevation above SWL. μ is a damping factor which varies linearly inside the sponge layer from zero at the beginning of the layer to μ_{max} at the open boundary (see Fig.1).

Ohyama and Nadaoka (1991) have found that if the value of the coefficient in Eq.9 ranges from 0.25 to 0.50 and the sponge layer width is more than one wave length, the coefficient of reflection from the sponge layer will be less than 2%. Eq.6 can represent the free surface inside and outside the sponge layer since $\mu = \partial \mu/\partial X = 0$ outside the layer and, hence, the equation is reduced to the original dynamic boundary condition.

Applying Green's theorem, the integral form of Eq.1 can be written as follows (Brebbia and Walker, 1980):

$$\alpha(q)\phi(q) + \int_s (\phi \frac{\partial G}{\partial n} - \frac{\partial \phi}{\partial n}G)ds + \iint_\Omega q * G \, d\Omega = 0 \qquad (10)$$

where $\alpha(q)$ and $\phi(q)$ are the internal boundary angle and velocity potential at point (q), respectively; s represents the outer boundary; and G is the Green's function defined as:

$$G = \ln(1/r) + \ln(1/R) \qquad (11)$$

where r is the distance between the point of interest (q) and other domain points and R is the distance between the point (q) and the image of other domain points considering the seabed as a mirror line.

The weighted residual method has been applied to integrate the dynamic boundary condition on the free surface using linear elements and weighting factor ϖ resulting in the following integral equation.

$$\int \varpi \left\{ \frac{\partial \phi}{\partial t} + 0.5 \left(n_z^2 \left[\frac{\partial \eta}{\partial t} \right]^2 + \left[\frac{\partial \phi}{\partial s} \right]^2 \right) + g\eta + \mu\phi - \int \frac{\partial \mu}{\partial X} \phi dX \right\} ds = 0 \quad (12)$$

Further details about this method are given in Ohyama and Nadaoka (1991).

Initial condition:

The water surface elevation above the SWL, the velocity potential and their time derivatives are set to zero at the initial time step of the program (cold start). The model ramps up from this condition. Iterations for the location of the nonlinear water surface are made at each time step in a time marching scheme.

Porous Media

The flow in the porous media is considered to be rotational and the porewater is assumed to be incompressible but viscous. The continuity equation and the equations of motion (McCorquodale and Hannoura, 1978) for the flow inside the porous media are as follows:

$$\frac{\partial U}{\partial X} + \frac{\partial W}{\partial Z} = 0 \quad (13)$$

$$A\frac{\partial U}{\partial t} + BU\frac{\partial U}{\partial X} + CW\frac{\partial U}{\partial Z} + D^{\backslash}\frac{\partial P}{\partial X} + EU + FU\sqrt{U^2 + W^2} = 0 \quad (14)$$

$$A\frac{\partial W}{\partial t} + BU\frac{\partial W}{\partial X} + CW\frac{\partial W}{\partial Z} + D^{\backslash}\frac{\partial P}{\partial Z} + EW + FW\sqrt{U^2 + W^2} = 0 \quad (15)$$

where

$$A = \frac{\left(1 + \frac{1-m}{m}C_{AX}\right)}{mg}, \qquad B = C = \frac{1}{m^2g}, \qquad D^{\backslash} = \frac{1}{\gamma}, \quad E = \frac{4.6\upsilon}{gmD^2}$$

$$F = \frac{0.79}{gm^{1/2}D}, \quad P = p + \gamma Z$$

and U,W,P are the horizontal and vertical water particle velocities and the porewater pressure, respectively; p is the dynamic porewater pressure; C_{AX} is the added mass coefficient; g is the acceleration of gravity; υ is the kinematic viscosity of water; γ is the unit weight of water; and D is the mean particle diameter.

The porous media equations are subjected to the following boundary conditions:

$$P = -\frac{\partial \phi}{\partial t} - \frac{1}{2}\left\{\left(\frac{V_n}{m}\right)^2 + V_s^2\right\} - \gamma Z \qquad \text{(on } S_s) \quad (16)$$

$$V_n = (W\cos\theta \pm U\sin\theta) \qquad \text{(on } S_s) \quad (17)$$

$$V_s = \frac{\partial \phi}{\partial S} \qquad\qquad\qquad\qquad (\text{on } S_s) \quad (18)$$

$$V_n = 0 \qquad\qquad\qquad\qquad (\text{on } S_b) \quad (19)$$

where V_s is the water particle velocity in the tangential direction to the boundary and θ is the inclination of the permeable boundary on the X axis.

The continuity of the normal velocity component (V_n) and the porewater pressure have been considered along the surface boundary of the submerged breakwater. The tangential component of the water velocity along the breakwater surface has been solved using the Finite Difference Method (FDM).

The FEM in the porous media is based on the weighted residual method. A special isoparametric trapezoidal element has been considered for discretization of the FEM domain. A four node element for the velocity (u and w) and eight node element for the pressure (p) have been employed to solve the problem. Linear interpolation and weight functions have been used for the continuity equation but a special technique has been applied to the equations of motion (Mizutani et al., 1995).

Initial conditions:
The velocity, pressure and their derivatives have been set to zero at the initial time step of the program (cold start) and a time marching scheme has been used to compute the flow inside the porous media at subsequent steps.

BEM-FEM Model Development
The BEM model for the simulation of the wave motion and the FEM model for porous flow have been linked together into one model that computes simultaneously the wave deformations outside the breakwater and the porous media flow inside the breakwater. The time derivative of any variable ψ at any time step (n) in the porous media or the wave field equations is solved using Taylor series expansion as follows:

$$\left(\frac{\partial \psi}{\partial t}\right)^n = 2\frac{\Delta\psi}{\Delta t} - \left(\frac{\partial \psi}{\partial t}\right)^{n-1} \qquad\qquad (20)$$

The nodes along the surface boundary of the breakwater and the water surface are located at spacing less than L/20 (where L is the wave length). The location of the FEM nodes are selected to be the same as that of the BEM along the interface between the breakwater and the wave domain. The time step of the model is initially selected to be T/24 and then the results are compared to the experimental results. If the difference between the numerical and experimental results is more than an accepted tolerance, smaller time steps are selected. It has been found that time increments less than T/24 may be needed for steep waves.

PHYSICAL MODEL

Submerged breakwater experiments were conducted in the coastal engineering laboratory at Nagoya University. These experiments measured the wave forces on spherical armor units (Fx and Fz), wave deformations and the water velocity around the surface of the breakwater. The submerged breakwater was constructed of spherical glass balls 3.0 cm in diameter and placed in a wave tank of 25.0 m long and 0.70 m wide. The breakwater had a crown width of 220 cm, height of 21 cm, and the seaward face had a slope of 3.2 (horizontal) : 1 (vertical). The balls were arranged to produce the maximum densely packed arrangement and their computed corresponding porosity was 26%. Two possible positions were considered for the spheres, namely, embedded and non-embedded positions (Mizutani et al., 1992). The experiments were conducted in a water depth of 28.0 cm so that the still water depth over the crown was 7.0 cm. Wave heights (H) of 3.0, 5.0, 7.0 and 10.0 cm and wave periods (T) of 1.0, 1.40 and 1.80 sec were examined. Records were sampled for one minute at a rate of 50 hz.

It was observed that the waves pass over the breakwater without breaking for wave heights 3.0 and 5.0 cm, but break for larger heights. Studies were formerly conducted to estimate the wave forces on armor units over a submerged breakwater and proved that the dimensionless non-breaking wave force, normalised by the wave height, on the armor is higher than the breaking one (Mizutani et al., 1992). Therefore, the non-breaking wave conditions will only be used for comparison and discussions in this study.

ESTIMATION OF WAVE FORCES

Standard Morison type equations have been found to be generally applicable to estimate the horizontal wave forces on the spherical armor units of submerged breakwaters (Rufin et al., 1996). However, in this study, the wave force has been considered to be composed of three components as follows:

$$F_x = \frac{1}{6}C_{MX}\rho\pi D^3 \frac{\partial u_r}{\partial t} + \frac{1}{8}C_{DX1}\rho\pi D^2 u_r \sqrt{u_r^2 + w_r^2} + 3C_{DX2}\rho v\pi D u_r \qquad (21)$$

By applying Eq.21, the horizontal wave force acting on a small element of a homogeneous porous submerged breakwater can be written as follows:

$$F_x = \rho V C_{MX}\frac{\partial u_r}{\partial t} + \frac{1}{2}C_{DX1}\rho A_x u_r \sqrt{u_r^2 + w_r^2} + C_{DX2}\frac{3\rho v S}{D}u_r \qquad (22)$$

where u_r and w_r are the porewater velocity components in the horizontal and vertical directions, respectively; S is the surface area of the armor unit affected by friction with the flow; ρ is the porewater density; C_{MX} is the coefficient of mass; and C_{DX1} and C_{DX2} are the drag coefficients in the X direction. A_x is the projected area of the armor unit in the X direction and V is its volume. This form of the Morison equation includes the common inertia and quadratic drag terms but also has a linear drag term. This linear term is analogous to Darcy flow in groundwater.

To solve the modified Morison equation, the porewater velocities (u_r , w_r), V, S and A_x have been expressed as follows and inserted into Eq.22.

$$A_x = (1-m)\Delta Z \tag{23}$$

$$V = (1-m)\Delta X \Delta Z \tag{24}$$

$$S = 2(1-m)\Delta X \tag{25}$$

$$u_r = \frac{U}{m}, \; w_r = \frac{W}{m} \tag{26}$$

where ΔX, ΔZ are the horizontal and vertical dimensions of the computational unit, respectively. Therefore, Eq.22 can be now expressed in terms of the flow parameters inside the porous media and the computational unit size as follows:

$$F_x = \rho \frac{(1-m)}{m} C_{MX} \frac{\partial U}{\partial t}\Delta X \Delta Z + \tfrac{1}{2}C_{DX1}\rho\frac{(1-m)}{m^2}U\sqrt{U^2+W^2}\,Z + C_{DX2}\frac{3\rho vS}{D}U \tag{27}$$

Furthermore, the force per unit weight of the porewater (f_x) can be expressed as follows:

$$f_x = \frac{(1-m)}{gm^2}C_{MX}\frac{\partial U}{\partial t} + \frac{C_{DX1}(1-m)}{2m^3 g \Delta X}U\sqrt{U^2+W^2}\,\Delta Z + \frac{3C_{DX2}v}{gmdD}U \tag{28a}$$

$$d = \frac{m\Delta X \Delta Z}{S} \tag{28b}$$

By comparing Eq.28 with the horizontal equation of motion in the porous media (Eq.14), the coefficients E and F are now modified and can be expressed as follows:

$$E = \frac{3C_{DX2}v}{gmdD} \tag{29a}$$

$$F = \frac{C_{DX1}(1-m)}{2m^3 g \Delta X} \tag{29b}$$

The size of the computation unit should be selected such that the side length is not less than D and, therefore, the value of $\Delta X = \Delta Z = D$ has been used in Eq.29 to compute the resistance coefficients as shown in Eq.30. Consequently, the coefficients C_{MX} , C_{DX1} and C_{DX2} should be first estimated in order to be able to use the modified equations of motion.

$$E = \frac{6(1-m)C_{DX2}v}{gm^2 D^2} \tag{30a}$$

$$F = \frac{C_{DX1}(1-m)}{2m^3 gD} \tag{30b}$$

ESTIMATION OF THE RESISTANCE COEFFICIENTS

Using the experimentally measured values of the wave forces and water velocities, the values of the coefficients (C_{MX}, C_{DX1} and C_{DX2}) have been estimated for the previously described wave conditions by means of the least square technique applied to Eq.21. The corresponding values of these coefficients for the case of non-embedded spheres have been plotted against, the Keulegan-Carpenter number, KC_x in Figs. 2-4. The KC_x number is U_mT/D where U_m is the maximum horizontal porewater velocity. Also shown are the data for the case of isolated spheres by Iwata and Mizutani (1989).
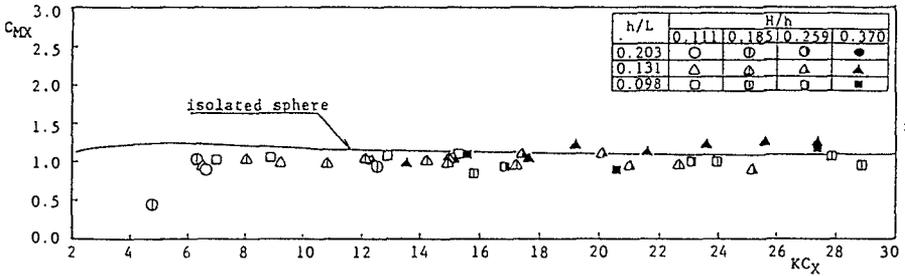
Fig.2 Coefficient of mass (C_{MX}) versus KC_x
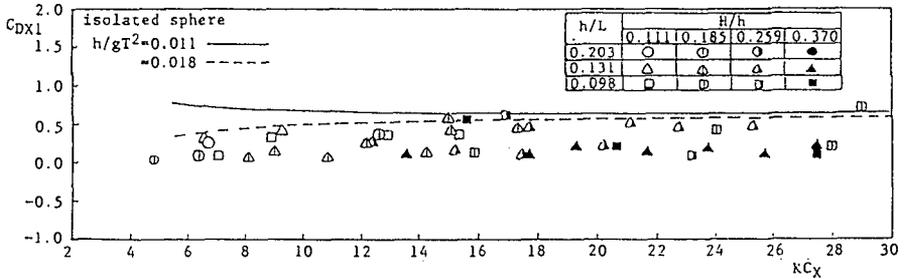
Fig.3 Coefficient of drag (C_{DX1}) versus KC_x
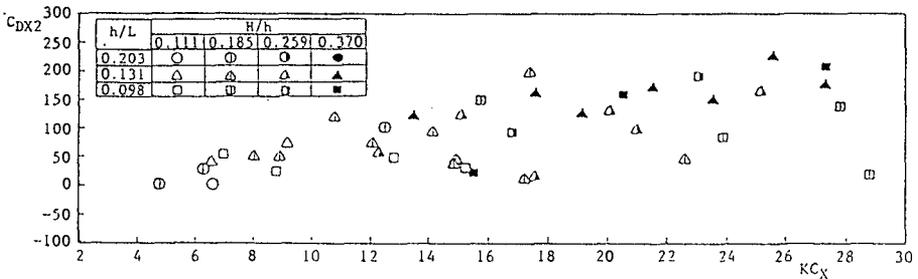
Fig.4 Coefficient of drag (C_{DX2}) versus KC_x

It is clear in Fig.2 that the value of C_{MX} is almost constant and independent of KC_x. Also, the values for isolated spheres and armor spheres are very similar. The value of C_{MX} has been estimated to be 0.96 (C_{AX}= -0.04) by taking the average over all computed values. This value has been used in the numerical model for comparison with the experiment.

The value of C_{DX1} ranges from 0.20 to 0.60 and is only weakly dependent upon KC_x as shown in Fig.3. The values of C_{DX1} for isolated spheres are generally higher than that for the armor units of a submerged breakwater. It is worth mentioning that the coefficient of drag C_{DX1} , formerly estimated by a standard Morison type equation and neglecting the linear friction term, experienced large scatter at small values of KC_x (Rufin et al., 1996). It has been estimated that C_{DX1} = 0.45 for use in the numerical model computations by taking the average over all the computed values.

The experimental results for C_{DX2} show large scatter, especially at large KC_x. The range is from a minimum of near zero for low KC_x to a maximum near to 200 for high KC_x. However, it has been found that the relative importance of the linear friction term including the drag coefficient C_{DX2} is very small at values of $KC_x > 10$, where flow separation occurs. Its effect is only considerable at low values of KC_x. Therefore, a value of C_{DX2}=25.0 has been estimated for use in the numerical model by considering the average of its computed values for the range of KC_x<10.0.

RESULTS AND DISCUSSIONS

The BEM-FEM model, employing modified resistance coefficients and their experimentally estimated values, has been used to model waves over a submerged breakwater. The comparisons with experimental results confirm the importance of the modified coefficients.

A velocity vector diagram and the wave profile along the wave tank at t/T=5.0 are shown in Fig.5. It is obvious that the water flows into the breakwater at the locations of the wave crests and flows out of it at locations of the wave trough. The areas over the leading edge of the crown and on the offshore slope have higher velocities than the other locations inside the breakwater. There is a rapid change in the free surface as the waves encounter the structure.

_ 1CM/S
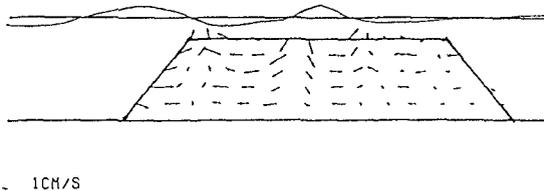
Fig.5 Wave deformation around and water velocity inside the breakwater at
t/T=5.0 (h/gT^2 = 0.029, H/h = 0.11)

The computed and measured water surface levels over the crown of the breakwater at X/L=0.30 and X/L=0.50 for a wave height (H) 3.0 cm and period (T) 1.40 sec are plotted in Fig.6. The BEM-FEM model agrees well with the measured water levels along the crown of the submerged breakwater. The waves are very nonlinear and asymmetric. Computations have also been conducted to evaluate the average wave setup ($\bar{\eta}$) at X/L=0.30 and 0.50 over the crown. It is obvious that the differences between the BEM-FEM model results and the experiment are small (Fig.6).
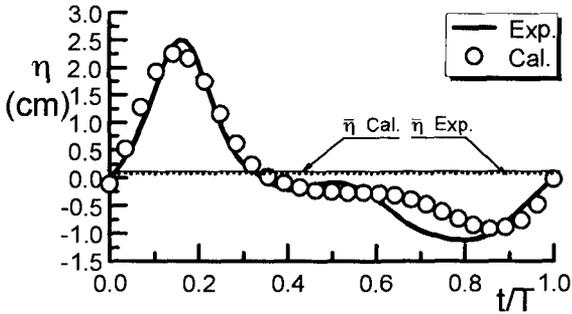
Fig.6a Free surface elevation at X/L=0.30 over the crown
($h/gT^2 = 0.015$, $H/h = 0.11$)
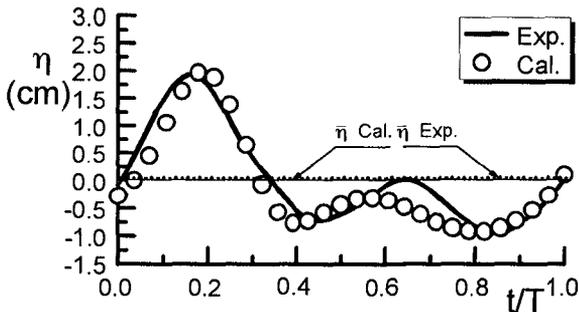
Fig.6b Free surface elevation at X/L=0.50 over the crown
($h/gT^2 = 0.015$, $H/h = 0.11$)

The value of η_{rms} along the wave tank has been used to represent the wave energy and comparison has been made between its measured and computed values along the wave tank (Fig.7). The measured and computed values are in good agreement. A partial standing wave is formed offshore of the breakwater and nonlinear wave damping occurs across the crown leading to a small transmitted wave to the lee side.
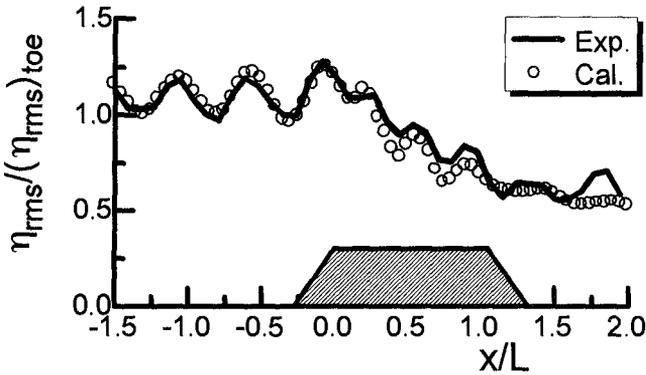
Fig.7 water level variation along the wave tank ($h/gT^2 = 0.015, H/h = 0.11$)

The computed and measured values for the maximum water particle velocity components (U_m and W_m) along the crown of the breakwater are shown in Fig.8. While U_m has been used to denote the maximum horizontal porewater velocity over the crown, W_m has been used to express the maximum vertical seepage velocity along it. The results are compared for a wave height (H) of 3.0 cm and period (T) of 1.0 sec. It can be observed that the numerical model results agree qualitatively well with the experimental ones. However, the values computed by the numerical model seem to be higher than that in the experiment. The velocities have been measured in the experiment at a small distance over the crown but, in the BEM-FEM model, the velocities have been computed exactly on the crown surface. It has been found that the locations of the maximum horizontal and vertical velocities are located at the offshore crown corner of the breakwater. This is in agreement with earlier investigations that have also proved experimentally that the point of maximum wave force is at the same location (Mizutani et al., 1992).
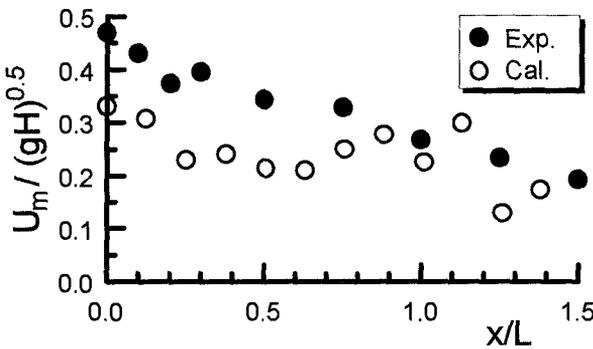

Fig.8a Maximum horizontal porewater velocity along the crown
($h/gT^2 = 0.029, H/h = 0.11$)
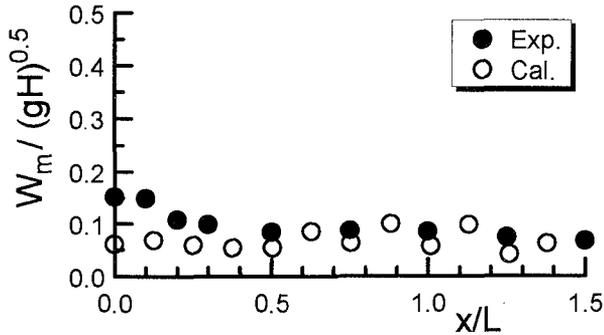
Fig.8b Maximum vertical seepage velocity along the crown
$(h/gT^2 = 0.029, H/h = 0.11)$

CONCLUSIONS AND PERSPECTIVES

1) A numerical model is presented which simulates the nonlinear interaction between free surface waves and a submerged permeable breakwater. Modified resistance coefficients have been developed from experimental measurements and improved the results of the BEM-FEM model.

2) The model accurately predicts the partial standing wave that is formed offshore of the breakwater and the damping which occurs along it causing a small wave to be transmitted to the lee of the breakwater. The model can accurately estimate the transmitted wave height resulting from the combined effects of reflection, shoaling and dissipation.

3) The numerical model has been shown to compute with good accuracy the wave kinematics inside and around the submerged breakwater. Therefore, this model can be used further for studying the stability of the armor of the breakwater.

4) The point of maximum velocity along the submerged breakwater is at the offshore corner of the crown for all wave conditions tested in this study. As a result, the location of the maximum wave forces on the armor units is also at the offshore crown corner.

5) The model may be used to optimize the submerged breakwater shape, size and properties for site specific design requirements.

ACKNOWLEDGEMENT

REFERENCES

Brebbia, C. A. and Walker, S. (1980). *Boundary element techniques in engineering*, Butterworths, London.

Brorsen, M. and Larsen, J. (1987). *Source generation of nonlinear gravity waves with the boundary integral equation method*, Coastal Eng. 11, pp. 93-113.

Cruz, E.C., Isobe, M. and Watanabe, A. (1992). *Nonlinear wave transformation over a submerged permeable breakwater*, Coastal Eng. 23, ASCE, pp. 1101-1114.

Gu, G. Z. and Wang, H. (1992). *Numerical modelling for wave energy dissipation within porous submerged breakwaters of irregular cross section*, Coastal Eng. 23, ASCE, pp. 1189-1202.

Hannoura, A.A. and McCorquodale, J.A. (1985). *Rubble mounds: numerical modelling of wave motion*, J. WatWay, Port, Coastal Ocean Eng., ASCE 111, pp. 800-816.

Iwata, K. and Mizutani, N. (1989). *Experimental study on wave force acting on a submerged sphere*, Proc. of 8th Conf. on Offshore Mechanics and Arctic Eng., OMAE, pp.145-152.

McCorquodale, J.A. and Hannoura, A.A. (1978). *Hydraulic conductivity of rockfill*, J. Hydraulic Research, No. 2, pp. 123-137.

Mizutani, N., Iwata, K., Rufin, T.M., Jr. and Kurata, K. (1992). *Laboratory investigation on the stability of a spherical armor unit of submerged breakwater*. Coastal Eng. 23 , ASCE, pp.1400-1413.

Mizutani, N., Rufin, T.M.Jr. and Iwata, K. (1994). *Stability of armor stones of a submerged wide-crown breakwater*, Coastal Eng. 24 , ASCE, pp.1439-1453.

Mizutani, N., Goto, T. and McDougal, W. (1995). *Hybrid-type numerical analysis of wave transformation due to a submerged permeable structure and internal flow*. Proc. of Coastal Eng., JSCE, Vol. 42(1), pp.776-780. (in Japanese)

Ohyama, T. and Nadaoka, K. (1991). *Development of a numerical wave tank for analysis of nonlinear and irregular wave field*, Fluid Dynamics Research 8, pp. 231-251.

Rufin, T.M. Jr., Mizutani, N. and Iwata, K. (1996). *Estimation method of stable weight of spherical armor unit of a submerged wide-crown breakwater*, Coastal Eng., Elsevier, Vol.28, pp. 183-228

Sakakiyama, T., Kajima, R., and Abe, N. (1991). *Numerical simulation of wave motion in and near breakwaters*, Proc. of Coastal Eng., JSCE, Vol.38(2), pp. 545-550. (in Japanese)

Sakakiyama, T. (1992). *Numerical analysis of wave disintegration due to submerged breakwaters*, Proc. of Coastal Eng., JSCE, Vol. 39(2), pp. 626-630. (in Japanese)